Abhath Journal of Basic and Applied Sciences., 2(2) (2023) 1-14

Abhath Journal of Basic and Applied Sciences

Website:https://ojs.abhath-ye.com/index.php/OJSRJBAS/about

doi: https://doi.org/10.59846/ajobas.v2i2.483

Research paper, Short communication, Review, Technical paper

FT-IR, NMR spectral analysis and theoretical NBO, FMOs, UV-Vis analysis of 7,7',8,8'-tetracyanoquinodimethane (TCNQ) in its ground and excited states by DFT and CIS methods

Sabah Yahya Huthaily*

Faculty Of Education ,Department Of Physics, Hodeidah University, Yemen

***Corresponding author E-mail:** s_huthaily@yahoo.com*

Received: 5 Oct 2023. Accepted: 23 Nov 2023. Published 30 Dec 2023.

Abstract

The Gaussian 03W program has been used for theoretical computations to compute optimal geometry, nuclear magnetic resonance (NMR), vibrational frequencies, natural atomic charges, natural bond orbital,(NBO), frontier molecular orbitals (FMOs), Ultraviolet-Visible (UV-Vis) analysis at DFT/B3LYP/6-31G(d) and ab initio CIS/6-31G(d) methods for 7,7',8,8'-tetracyanoquinodimethane (TCNQ) ($C_{12}H_4N_4$) in the ground as well as in the excited states. The ^1H, ^{13}C and ^{15}N NMR and further research is done on other molecular characteristics. The scaled vibrational frequencies and published works have been compared. The title molecule's infrared spectra are provided with a complete interpretation. In addition, stability of the molecule arising from hyperconjugative interactions. NBO analysis has been used to analyze charge delocalization. The findings demonstrate that charge in electron density (ED) in the π^* anti- bonding orbitals and $E^{(2)}$ energies verifies that intra-molecular charge transfer (ICT) is occurring within the molecule. The highest occupied molecular orbitals (HOMOs) and the lowest unoccupied molecular orbitals (LUMOs) energies that were computed demonstrate that charge transfer takes place inside the molecule.. Finally, the UV-Vis spectrum was measured in gas phase.

Keywords: *TCNQ, DFT, CIS, molecular structure, NMR, vibrational asssignement, natural atomic charge, NBO, FMOs, UV-Visible analysis.*

1. Introduction

Crystalline organic materials, or MOMs, are soft solids which involve organic molecules arranged in a three-dimensional periodic distribution with weak intermolecular force. Dipolar (permanent or fluctuating) charges and hydrogen bonding, and π-π interactions basically mediate the transition among molecules [1]. Additionally, organic materials are beginning to show promise as materials for solar cells, photodiodes, transistors, and (bio)chemical sensors [2–5]. One important factor is the effectiveness of charge transmission in the organic layer(s) plays a key role [6].

In materials research, charge-transfer (CT) systems are currently of great importance. These systems can be found in organic semiconducting polymers or in molecular optoelectronic devices including molecular-based transistors, wires, and rectifiers [7-10]. As a powerfully electron acceptor, highly polar molecule, 7,7',8,8'-tetracyanoquinodimethane (TCNQ) ($C_{12}H_4N_4$) is frequently utilized to create highly conducting charge-transfer complexes [11-14]. TCNQ is known to form CT complexes with many aromatic hydrocarbons [15].

Molecular force fields produced by the density functional theory (DFT) approach, which takes into account local or non-local functional, are extremely consistent with experimental results. The Becke's three-parameter exchange functional (B3) [16] and the Lee, Young, and Parr correlation functional (LYP) [17] were combined to create the B3LYP [16-18] approach, which is selected to perform the calculations. GaussView 4.1[19] tool, a molecular visualization, is used to perform all of the computations. An effective method for predicting the characteristics of electronically excited states of aromatic molecules is the configuration interaction singles (CIS) method used in ab initio molecular orbital computations [20], which were recently introduced. The application of this computational method was effective in predicting the vibrational frequencies and molecular geometries of benzene in its electrically excited states [21].

The primary goal of this work is to identify theoretical approaches that provide a greater degree of accuracy when determining vibrational wavenumbers and molecular structural characteristics.. In addition to this, the NMR, FMOs, NBO analysis, UV-Vis spectrum have been used to elucidate the information regarding charge transfer within the molecule.

2. Computational methods

A Pentium IV personal computer with 2.8 GHz processor and 256 MB RAM was utilized to run all the calculations. The Gaussian 03W program package[22]. was used to do the calculations.

In this study, the DFT approach (B3LYP) and CIS methods adopting split valence 6-31G(d) besis set has been applied to the computation of vibrational frequencies, molecular structure, nuclear magnetic resonance (NMR), ultraviolet-visible (UV-Vis) spectrum, natural bond orbitals (NBO), chemical hardness (η), chemical potential (μ), thermodynamic properties, and energies of the TCNQ molecule in its ground state (S_o) as well as in its excited state (S_1). Without any restrictions, the potential energy surface had minimal geometry created using standard geometrical. Vibrational frequency calculations at the DFT level were performed using the optimized structural parameters, which allowed all stationary points to be characterized as minima. Then, harmonic vibrational frequencies were calculated using vibrationally averaged nuclear locations of TCNQ, yielding IR frequencies and their intensities. The CIS method was used for modeling the electronically excited states in the frozen core approximation. One of the few Ab initio methods for optimizing the geometry of molecules in their excited states is the CIS method. With a minimal demand on computer resources, it offers analytical first and second derivatives that allow geometrical optimizations in the electronically excited state [20]. The NBO calculations were carried out using the NBO 3.1 [23] program as implemented in the Gaussian 03W [22] package at the DFT/B3LYP/6-31G(d) and CIS/6-31G(d) levels in order to understand various second order interactions between the filled orbitals of one subsystem and

unoccupied orbitals of another subsystem, which is an indicator of hyper conjugation or intermolecular delocalization.

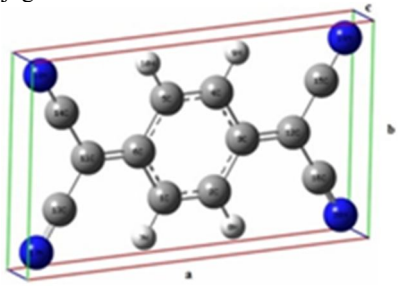

Figure 1 Phase diagram of carbon dioxide.

3. Results and discussion

3.1. Molecular geometry

Theoretical crystal structural simulations of TCNQ molecule at room temperature show a triclinic shape with space group P1 and lattice parameters $a = 9.3760\,Å$, $b = 5.4290\,Å$ and $c = 1.0121\,Å$ (see Figure 1). The TCNQ molecule's optimal structural parameters were determined at the B3LYP/6-31G(d) and CIS/6-31G(d) levels, for both the S_o and S_1 states, respectively, are mentioned in Table 1. This molecule's crystal structure is unavailable, hence the structure that is optimal only be compared to other comparable systems whose configurations have also been optimized [24-26]. For instance, the range of 1.3598-1.4498 Å for B3LYP/6-31G (d) method in the ground state, which corresponds to the optimal bond lengths of C–C in the phenyl ring, is in good agreement with the literature [26] for phenyl ring 1.3782-1.4205 Å. In these species, there are three different kinds of CC bonds: strained C=C, double C=C, and single C–C bonds. The current molecule is made up of two methylene groups that are connected to one phenyl ring by four cyano (nitrile) groups. Since the molecule under study has C1 point group symmetry, no species distribution would be meaningful for C_1 point group.

Ring C=C, C-H, and C≡N bond lengths drop as a result of the primary electronic excitation from the S_0 to the S_1 state, which is a reduction in the aromatic ring as seen in Table 1. The angles $\angle C2C1C6$, $\angle C1C2C3$, $\angle C3C4C5$ and $\angle C4C5C6$ tighten down by about 0.03^0 due to the π-electron interaction between the aromatic ring and the NCC group while $\angle C2C3C4$ and $\angle C1C6C5$ to open up by 0.06^0. The planar TCNQ molecule in the S_1 state has a slightly different ring geometry than a perfect hexagon.

3.2. NMR calculation

When attempting to identify reactive ionic species, the isotropic chemical shifts are commonly utilized. It is acknowledged that valid computations of magnatic characteristics depend on precise predictions of molecular geometries [27]. Using the 6-31G(d) basis set and the B3LYP approach, the molecular structure of TCNQ is optimized in this work. Then, using the GIAO technique, the ^1H, ^{13}C and ^{15}N chemical shifts were computed at the same theoretical level [28]. The GIAO was applied more effectively when the procedure was successfully applied to the ab initio self-consistent file (SCF) computational, using techniques drawn from analytic derivatives methodology, greatly enhanced the application of the GIAO [29] approach to molecular systems. Due to its quicker convergence of the computed properties upon expanding the basis set, the GIAO approach is considerably better [30].

Tables 2(a, b and c) provide the theoretical values for ^1H, ^{13}C and ^{15}N NMR of TCNQ molecule. The calculation reported here were performed in gas phase. Chemical shifts were reported in part per million (ppm). The ^1H, ^{13}C and ^{15}N NMR chemical shifts are shown in Figure 2. The NMR spectra for proton, carbon and nitrogen atoms show degenerate peaks which are condensed together (degeneracy tolerance 0.05).

Table 1 Optimized geometrical parameters, bond length (Å) and angle (◦), for TCNQ molecule in its ground (S_0) and excited (S_1) states calculated by B3LYP/6-31G(d) method.

Parameters	Ground state (S_0)	Excited state (S_1)
Bond length (Å)		
C1-C2	1.3598	1.3609
C1-C6	1.4498	1.4301
C1-H7	1.0840	1.0712
C2-C3	1.4498	1.4301
C2-H8	1.0840	1.0712
C3-C4	1.4498	1.4301
C3-C12	1.3933	1.4121
C4-C5	1.3598	1.3609
C4-H9	1.0840	1.0712
C5-C6	1.4498	1.4301
C5-H10	1.0840	1.0712
C6-C11	1.3933	1.4121
C11-C13	1.4250	1.4113
C11-C14	1.4250	1.4113
C12-C15	1.4250	1.4113
C12-C16	1.4250	1.4113
C13-N17	1.1756	1.1528
C14-N18	1.1756	1.1528
C15-N19	1.1756	1.1528
C16-N20	1.1756	1.1528
Bond angle (°)		
C2C1C6	121.2135	121.1813
C2C1H7	120.1065	119.4766
C6C1H7	118.6800	119.3422
C1C2C3	121.2135	121.1813
C1C2H8	120.1065	119.4766
C3C2H8	118.6800	119.3422
C2C3C4	117.5730	117.6374
C2C3C12	121.2129	121.1813
C4C3C12	121.2141	121.1812
C3C4C5	121.2135	121.1813
C4C3H9	118.6801	119.3422
C5C4H9	120.1064	119.4765
C4C5C6	121.2135	121.1813
C4C5H10	120.1064	119.4765
C6C5H10	118.6801	119.3422
C1C6C5	117.5730	117.6374
C1C6C11	121.2129	121.1813
C5C6C11	121.2141	121.1812
C6C11C13	121.6423	121.1623
C6C11C14	121.6414	121.1623
C13C11C14	116.7163	117.6753
C3C12C15	121.6414	121.1623
C3C12C16	121.6423	121.1623
C15C12C16	116.7163	117.6753
C11C13N17	179.8153	179.9905
C11C14N18	179.7709	179.9875
C12C15N19	179.7709	179.9875
C12C16N20	179.8156	179.9906

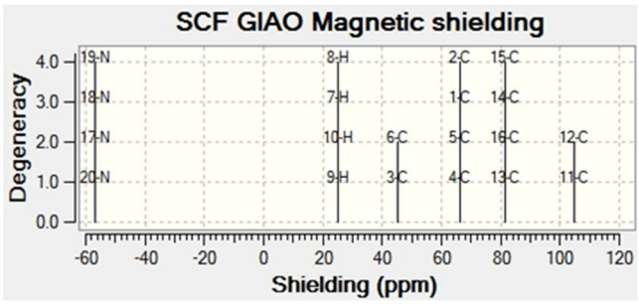

Figure 2 The calculated ^1H, ^{13}C and ^{15}N NMR spectra of TCNQ molecule.

In this work, the calculated proton NMR chemical shifts show only one proton peak at chemical shift 25.1169 ppm rather than four peaks (see Figure 2).[13]C NMR chemical shifts in the ring for the title molecule are in the range from 45.09215 to 104.5578 ppm, according to (Table 2b)'s expectations. There are twelve peaks in the chemical formula, but only four peaks with varying strengths may be seen in the carbon NMR spectrum. The conclusion is that symmetry exists, rendering certain carbon atoms identical.When the N atom, i.e. more electronegative property, bonds to the nearby carbon atom, it polarizes the electron distribution and lowers the electron density at the birdge of the molecule in question. In the present work, the nitrogen NMR chemical shifts show only one peak at -56.8395 ppm rather than four peaks as expected from the molecular formula.

Table 2a Calculated [1]H NMR chemical shifts (ppm) of the TCNQ molecule.

Atoms	Degeneracy	Shielding (ppm)
H7	4	25.1169
H8	4	25.1169
H9	4	25.1169
H10	4	25.1169

Table 2b Calculated [13]C NMR chemical shifts (ppm) of the TCNQ molecule**.**

Atoms	Degeneracy	Shielding (ppm)
C3	2	45.09215
C6	2	45.09215
C1	4	66.23815
C2	4	66.23815
C4	4	66.23815
C5	4	66.23815
C13	4	81.55370
C16	4	81.55370
C14	4	81.55370
C15	4	81.55370
C11	2	104.5578
C12	2	104.5578

Table 2c Calculated [15]N NMR chemical shifts (ppm) of the TCNQ molecule.

Atoms	Degeneracy	Shielding (ppm)
N17	4	-56.8395
N20	4	-56.8395
N18	4	-56.8395
N19	4	-56.8395

3.3. Vibrational assignments

There are 20 atoms in the TCNQ molecule and therefore contains 54 normal modes of fundamental vibrations. The 54 fundamental vibrations are fall into 37 in-plane vibrations of A' species and 17 out-of-plane vibrations of A''species, i.e., $\Gamma = 37\,A'$ (planar) + $17\,A''$ (non-planar). All the 54 fundamental vibrations are active in IR. The vibrational frequencies of the TCNQ in the S_0 state, calculated at the B3LYP level of theory using the double split valence basis 6-31G(d) are presented in Table 3. The calculated frequencies were scaled by a factor of 0.9608 [31]. Within each basic wavenumber, the estimated modes are numbered from the lowest to the largest frequency. Figure 3 shows the stick infrared (IR) spectrum of TCNQ molecule in the ground state calculated at DFT/B3LYP level using 6-31G(d) basis set. Molecular symmetry, reduced masses, force constant, and the specific motion of each individual atom are the primary factors considered when assigning each vibration. To verify the assignment, the computed frequencies are further checked with those published for additional benzene derivatives. Varsanyi and Szoke convention for benzene derivatives is followed for labeling the normal modes [32]. Table 3 demonstrates the induced IR intensity activity, reduces mass, and force constant of TCNQ molecule.

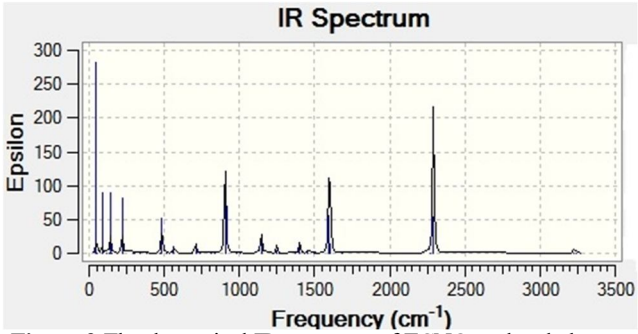

Figure 3 The theoretical IR spectrum of TCNQ molecule by DFT/B3LYP level at 6-31G(d) basis set.

Every vibrational mode was attributed to one of the nine motion types that the point group analysis anticipated: stretching, in-plane bending, out-of-plane bending, torsion, rocking, twisting, wagging, scissoring, butterfly [33].

3.3.1.C-H vibrations

Aromatic compounds exhibit one or more strong peaks between 3100 and 3000 cm^{-1} that are weak to medium in intensity. The type of the substituent has no discernible effect on the bands in this region [34]. The TCNQ molecule has four C-H moieties, making it a disubstituted aromatic system. The four anticipated C-H stretching vibrations that match the C1–H, C2–H, C4–H and C5–H units' stretching modes. The computed vibrations (mode nos. 54–51) by B3LYP/6-31G(d) method at 3113.828, 3111.691, 3096.883 and 3096.827 cm^{-1}, in this work, are attributed to C-H stretching vibrations and exhibit a similar agreement to those documented in previous studies [26,35].

Benzene and its derivatives' aromatic C-H in-plane bending vibrations are detected in the region 1300–1000 cm^{-1}. The bands are mild to medium intensity but still crisp [36]. The computed vibration (mode no. 38) by B3LYP/6-31G(d) level at 1215.309 cm^{-1} ,in this work, is attributed to the aromatic ring's C-H in-plane bending vibration, and the result is comparable to that found in published literature [26].

Typically, the 1000–675 cm^{-1} region is where absorption bands resulting from C–H out-of-plane bending vibrations are detected [37]. In this work, the computed vibrations (mode nos. 34, 33, 29, 28 and 25) by B3LYP/6-31G(d) level at 1008.784, 999.7697, 869.2360, 805.2704 and 681.667 cm^{-1} are attributed to C–H out-of-plane bending vibration of aromatic ring and the results are comparable to those documented in published literature [26].

3.3.2.Carbon vibrations

If the carbon double bonds (C=C) are conjugated with the ring, the vibrations become more interesting. The form of the substitution around the ring determines the actual positions more so than the substance of the substituents [38]. Raman and infrared bands appear in the region 1690-1560 cm^{-1} when a carbon double bond stretches.. In the infrared, the bands are frequently very weak or not visible at all. Low double bond C=C stretching frequencies are also observed in bridged rings with unsubstitude double bonds [34]. In this work, the computed vibrations (mode nos. 44, 37 & 36) by B3LYP/6-31G(d) method at 1535.313, 1199.689 and 1168.031 cm^{-1} are related to asymmetric stretching vibration of C=C bond while that computed vibration (mode no. 43) at 1442.501 cm^{-1} is related to symmetric stretching vibration of C=C bond. The computed vibrations (mode nos. 22, 21 &18) by B3LYP/6-31G(d) method at 595.9928, 594.9410 and 501.2849 cm^{-1} are related to in-plane bending vibration of aliphatic C-C-C while that computed vibration (mode no. 15) at 421.7900 cm^{-1} is related to out-of-plane bending vibration of aliphatic C-C-C.

3.3.3.C≡N vibrations

In comparison to saturated compounds, unsaturated or aromatic nitriles—where the double bond or ring is next to the carbon nitrogen C≡N group—absorb more strongly in the infrared spectrum, with the bands occurring at a slightly lower frequency around 2230 cm^{-1} [34]. In this work, the computed vibrations (mode nos. 50 & 49) by B3LYP/6-31G(d) method at 2201.317 and 2199.337 cm^{-1} are related to symmetric stretching vibration of C≡N group while that computed vibrations (mode nos. 48 & 47) at 2186.147 and 2186.093 cm^{-1} are related to asymmetric stretching vibration of C≡N group. Sundaraganesana et al. [39] claimed that, the C≡N stretching vibration of the benzonitrile compounds is computed at 2221 cm^{-1}. The theoretically computed vibrations (mode nos. 7 & 5) by B3LYP/6-31G(d) method at 135.4657 and 114.4504 cm^{-1} are assigned to in-plane bending vibrations of NC-C-C≡N group, while that computed vibration (mode no. 2) at 48.17711 cm^{-1} is related to out-of-plane bending vibration of NC-C-C≡N group.

3.3.4.Phenyl ring vibrations

Carbon-carbon (C – C) single bonds are the main type of ring modes in benzene. The benzene ring has six stretching vibrations, four of which are good group vibrations and have the highest magnitudes of wavenumbers, occurring close to 1600, 1580, 1490 and 1440 cm^{-1} are good group vibrations [40]. The bands tend to broaden the absorption zone with heavier substituents, shifting to somewhat lower wavenumbers and more substituents on the ring. The anticipated range for these vibrations is 1620–1260 cm^{-1} [40]. In this work, the computed C=C stretching vibrations (mode nos. 46, 45, 42 & 40) by B3LYP/6-31G(d) method at 1617.204, 1544.066, 1435.868 and 1346.967 cm^{-1} are related to the stretching vibrations of the skeleton carbon.

The region where the fifth ring stretching vibration is located, active nerar 1315±65 cm^{-1}, closely overlaps with the C-H in-plane deformation [40]. In this work, the computed C=C stretching vibrations (mode nos. 41, 39 & 35) by B3LYP/6-31G(d) method at 1397.149, 1320.507 and 1100.543 cm^{-1} are related to C=C stretching coupled with C–H in-plane bending vibration.

It has been reported that the ring breathing mode of para substituted benzene, with completely distinct substituents, is strongly IR active, with characteristic bands in the interval 850-780 cm^{-1} [32]. For the TCNQ molecule phenyl ring breathing mode calculated theoretically by the B3LYP/6-31G(d) method (mode no. 30) is predicted at 943.2986 cm^{-1}.

The theoretically computed vibrations (mode nos. 32, 31, 26 & 23) by B3LYP/6-31G(d) method at 986.6320, 962.6444, 706.1195 and 618.7186 cm^{-1} are related to in-plane bending vibrations of ring C-C-C, while that computed vibrations (mode nos. 27, 24, 17 & 14) at 780.8865, 630.3350, 465.9297 and 385.0637 cm^{-1} are related to out-of-plane bending vibration of ring C-C-C.

3.3.5. Lattice mode vibrations

"Lattice mode (butterfly)" is commonly referred to for frequency bands; these modes have been observed and calculated for a number of tiny and large molecular systems [41,42].In this work, these bands have been predicted at B3LYP/6-31G(d) level for title molecule (mode nos. 20, 19, 13-8, 6, 4, 3 & 1) at 542.1192, 516.4906, 365.7454-143.3070, 131.5546, 111.6536, 82.13168 and 47.00695 cm^{-1}.

3.4. Natural atomic charge

Atomic charge has been used to explain how chemical reactions produce electronegativity equalization and charge transfer [43]. In this work, the natural atomic charges, which shows the distribution of electron density, of TCNQ molecule in its ground and excited states are calculated by B3LYP/6-31G(d) and exhibited in Table 4. On the one hand, when TCNQ molecule is in its ground state the H9, H7, H10, H8, C3 and C6 atoms of TCNQ can accommodate higher positive charge and become more acidic. The bond lengths between C1-C2 and C4-C5 are exactly equal each other, 1.3598 Å. This observation supported the idea that the negative charge was delocalized through carbons C1, C2, C4 and C5. The atomic charges in the cyano group are almost identical in the molecules. On the other hand, the excited state of TCNQ molecule causes the positive charge of C3 and C6 becomes less positive (+0.128e) charge. As a consequence of excitation, the TCNQ molecule becomes less acidic. Overall, the nitrogen is the most negatively charged atom. The presence of C≡N bond leads to C11 and C12 become more acidic (i.e. high positive charge). Consequently, a change in the material's charge distribution will result from the application of electric [44]

Table 4 Natural atomic charges of TCNQ calculations performed at B3LYP/6-31G(d) level of theory.

Atom	Charge (a.u.)	
	S_0	S_1
C1	-0.134207	-0.163813
C2	-0.134206	-0.163813
C3	0.151859	0.023486
C4	-0.134207	-0.163813
C5	-0.134207	-0.163813
C6	0.151858	0.023486
H7	0.187391	0.275605
H8	0.187389	0.275605
H9	0.187393	0.275605
H10	0.187390	0.275605
C11	0.113716	0.153990
C12	0.113710	0.153990
C13	0.020454	0.041296
C14	0.020415	0.041295
C15	0.020528	0.041295
C16	0.020364	0.041296
N17	-0.206452	-0.241826
N18	-0.206359	-0.241825
N19	-0.206486	-0.241825
N20	-0.206344	-0.241826

3.5. Other features of TCNQ molecule

The TCNQ molecule's computed thermodynamic parameters in its S_0 and S_1 states are found by B3LYP/6-31G(d) level of theory and shown in Table 5. It has been suggested that scale factors be used in order to accurately anticipate the -point vibration energy (ZPVE), and the entropy, $S_{vib}(T)$ [45]. The differences in the ZPVE's see appear to be negligible. Moreover, the total energy and variations in the total entropy of TCNQ molecule at room temperature using the DFT and CIS approaches are also shown. The calculated dipole moment of the TCNQ in its ground and excited states are 0.0005 and zero (D), respectively. The dipole moment vector is actually oriented out of the ring plane in the y-direction (as seen from Figure 4). The small value of the dipole moment is attributed to low rearrangement of Mülliken charge [46]. The calculated self-consistent field (SCF) energies of TCNQ molecule in its ground and excited states are -678.382824056 Hrtree (-18459.88250 eV) and -674.162732632 Hrtree (-18345.04662 eV), respectively.

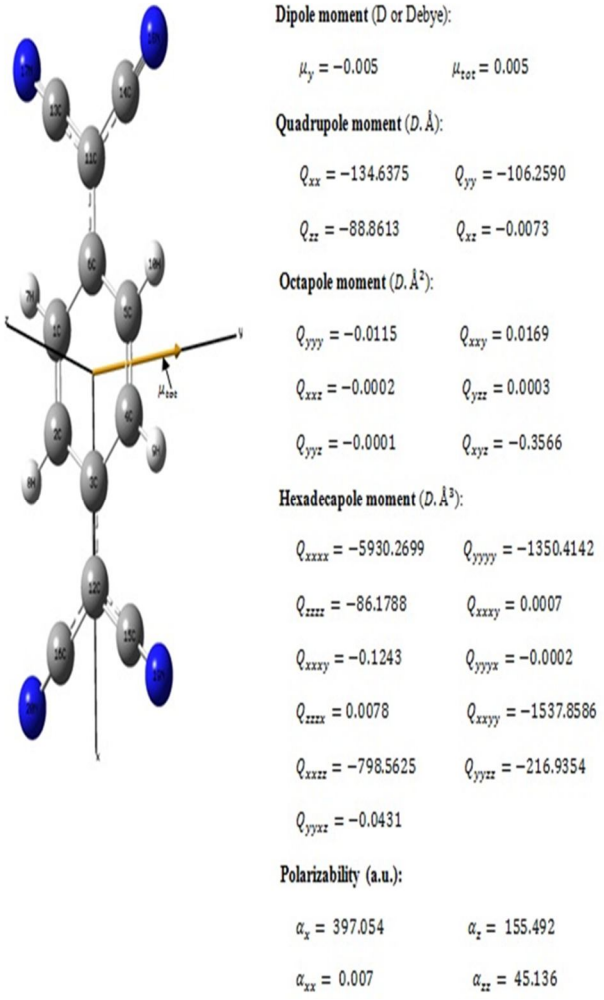

Figure 4 Some properties of TCNQ molecule in its ground state obtained from B3LYP/6-31G(d) calculations.

The chemical potential (μ) and chemical hardness (η) are defined as [47]:

$$\mu = \left(\frac{\partial E}{\partial N}\right)_{T,V} \qquad \eta = \frac{1}{2}\left(\frac{\partial^2 E}{\partial N^2}\right)_{T,V} \tag{1}$$

where E is the total energy, N is the number of electrons, T is the absolute temperature and V is the external potential. The highest occupied molecular orbital (HOMO) and the lowest unoccupied molecular orbital (LUMO) energies are used to compute these values, determined at B3LYP/6-31G(d) and CIS/6-31G(d) levels of theory using the expression:

$$\mu = -\left(\frac{IP+EA}{2}\right) \qquad \eta = \left(\frac{IP-EA}{2}\right) \tag{2}$$

where $IP = -E_{HOMO}$ and $EA = -E_{LUMO}$, IP and EA are the ionization potential and electron affinity of a molecule, respectively. In the present work, the calculated E_{HOMO}, E_{LUMO}, IP, EA, μ and η in the ground and excited states for TCNQ molecule are collected in Table 5. The electron affinity of TCNQ molecule in the ground state is 4.84339 eV which is high because TCNQ is a conjugated π –system, flat, extremely symmetrical molecule with four electron-withdrawing groups located at its different ends [48]. Whereas the value of electron affinity (2.77912 eV) in the excited state decreases may be due to the little charge distribution in the LUMOs orbitals of TCNQ molecule (see Fig. 5b). As a consequence, the excitation makes the TCNQ molecule becomes less acceptor.

Table 5 Theoretically computed energies (Hartree), zero-point vibrational energies (kcal mol^{-1}), rotational constants (GHz), entropies (cal mol^{-1} K^{-1}) and dipole moment (D), E_{HOMO} (eV), E_{LUMO} (eV), IP (eV), EA (eV), μ (eV), η (eV) and ΔE (eV) for TCNQ molecule in its S_0 and S_1 states.

Parameters	S_0	S_1
Total energy	-678.382824056	-674.162732632
Zero point energy	80.74244	86.08006
Rotational constants		
	1.15303	1.16162
	0.27118	0.27580
	0.21954	0.22288
Entropy		
Total	118.030	115.493
Translational	41.844	41.844
Rotational	32.815	32.776
Vibrational	43.370	40.873
Dipole moment	0.0005	0.0000
E_{HOMO}	-7.33652	-11.30479
E_{LUMO}	-4.84339	2.77912
IP	7.33652	11.30479
EA	4.84339	-2.77912
μ	6.08996	4.26284
η	-1.24657	-7.04196
ΔE	2.49313	7.50224

3.6. NBO analysis

Studying intra- and intermolecular bonding as well as bond interaction is made easier with the help of natural bond orbital analysis. Additionally, NBO offers a practical foundation for researching conjugative interaction or charge transfer in molecular systems. In the NBO study, the donor (i) level bonds to acceptor (j) level bonds interaction was assessed using the second order Fock matrix [49]. The estimation of the stabilization energy $E^{(2)}$ associated with the delocalization $i \rightarrow j$ for every donor (i) and acceptor (j) is:

$$E^{(2)} = \Delta E_{ij} = q_i \frac{F(i,j)^2}{\varepsilon_j - \varepsilon_i} \tag{3}$$

where q_i is the donor orbital occupancy, ε_i and ε_j are diagonal elements and $F(i,j)$ is the off diagonal NBO Fock matrix element. The more intense the interaction between electron donors and acceptors, the higher the energy $E^{(2)}$ value , i.e. the greater the degree of conjugation of the entire system and the stronger the tendency of electron acceptors to take electrons [50]. Electron density delocalization between occupied Lewis type (bond or lone pair) NBO and formally empty (anti bond or rydgberg) non-Lewis NBO is a representation of the stabilizing donor-acceptor interaction. In this work, NBO analysis has been performed to elucidate the intra-molecular and delocalization of the electron density within the TCNQ molecule in its ground and excited states at the DFT/B3LYP/6-31G(d) and CIS/6-31G(d) level, respectively. Because of the intra-molecular hyper conjugative interaction between σ (C1–C2) and σ^* (C1-C6), (C1-H7), (C2-C3), (C2-H8), (C3-C12) and (C6-C11), there is reduced stabilization of ~2.0 kJ/mol. Strong delocalization of 18.73 kJ/mol results from this improved further coupled with the anti bonding orbital of π^* (C3-C12) and (C6-C11). When electrons are donated from the σ (C4–C5) bond to σ^* (C3-C4), (C3-C12), (C4-H9), (C5-C6), (C5-H10) and (C6-C11), less stabilization of ~2.0 kJ/mol is achieved. This type of interaction energy is determined in the same way and is associated with the resonance in the molecule. 18.73 kJ/mol is strongly delocalized in electron density as a result of this improved further conjugate with the anti bonding orbital of π^* (C3-C12) and (C6-C11). Therefore, the most important interactions in the ground state of TCNQ molecule having maximum energy transfer are found from bonding orbitals (C1-C2) to anti bonding one (C3-C12) and (C6-C11) and from (C4-C5) to anti bonding (C3-C12) and (C6-C11) having strong stabilization

energy 18.73 kJ/mol. This study included a detailed discussion of the energy delocalization from these molecular bonds to other regions, which are indicated in Table 6a. Whereas in the excited state of this molecule, the stabilization energy of these donor bonds (C1-C2) and (C4-C5) increased from 18.73 to become 29.83 kJ/mol (Table 6b see appendix). The electron density (ED) of these donor bonds is slightly decrease from 1.98093 to 1.98002 e (Tables 6a & 6b see appendix). The interaction between lone pairs (LP) N17, N18, N19 and N20 with anti bonding (C11-C13), (C11-C14), (C12-C15) and (C12-C16) resulting stabilization energy to increase from 12.68 kJ/mole in the ground state to 13.52 kJ/mol in the excited state of TCNQ molecule, which denotes larger delocalization. As a consequence, $E^{(2)}$ energies confirms the occurrence of intra-molecular charge transfer (ICT) within the molecule.

3.7. Frontier molecular orbitals analysis

Frontier molecular orbitals (FMOs) are the most significant orbitals in a molecule. These orbitals are known as the highest occupied orbital (HOMO) and lowest unoccupied orbital (LUMO). The molecule's interactions with other species are dictated by these orbitals. The FMOs are crucial for the electrical and optical characteristics, chemical reactions, and UV-Vis spectra [51]. Characterizing the molecule's chemical reactivity and kinetic stability is aided by the frontier orbital gap. A molecule known as a "soft molecule" has a tiny frontier orbital gap, which makes it more polarizable and typically linked to high chemical reactivity and low kinitic stability [51]. Thus, the HOMO 's energy directly correlated with ionization potential(IP), but LUMO 's energy is directly tied to the electron affinity (EA). In the present work, the calculated values of HOMOs and LUMOs for TCNQ molecule in its ground and its excited states are collected in Table 7. According to the calculations, there are 52 occupied molecular orbitals in the TCNQ molecule. An essential stability component for structures is the energy gap (ΔE), which is the difference in energy between the HOMO and LUMO orbitals [52].

As seen from Table 7, the energy gap of TCNQ molecule increases from 2.49313 to 7.50224 eV by electric field effect. Furthermore, Figure 5(a and b) displays three-dimensional (3D) plots of HOMOs and LUMOs of TCNQ molecule in its ground and excited states, respectively. On the one hand, when the TCNQ molecule in its ground state, the HOMO, HOMO-2, HOMO-3, LUMO, LUMO+1 and LUMO+3 are concentrated on nearly the entire molecule, while the HOMO-1 and LUMO+2 are localized on the benzene ring (see Figure 5a). On the other hand, when the TCNQ molecule in its excited state, the HOMO and HOMO-1, are localized on C-C and C=C bonds, the HOMO-2, HOMO-3, LUMO+2 and LUMO+3 are localized on C=C and C-H bonds, while LUMO and LUMO+1 are localized on C=C and C≡N bonds. The fact that both the HOMOs and the LUMOs are primarily found on the rings suggests that the HOMO–LUMO orbitals are primarily of the π-anti bonding type [53].

Table 7 The calculated HOMOs (eV), LUMOs (eV) and energy gap (eV) of TCNQ molecule in its ground and excited states by DFT/B3LYP and ab initio CIS levels using 6-31G(d) basis set.

States	Ground state (eV)	Excited state (eV)
LUMO+3	-1.12983	3.80255
LUMO+2	-1.69692	3.80255
LUMO+1	-1.74481	2.77912
LUMO	-4.84339	2.77912
HOMO	-7.33652	-11.30479
HOMO-1	-8.99833	-11.30479
HOMO-2	-9.44297	-11.37717
HOMO-3	-10.14204	-11.37717
ΔE	2.49313	7.50224

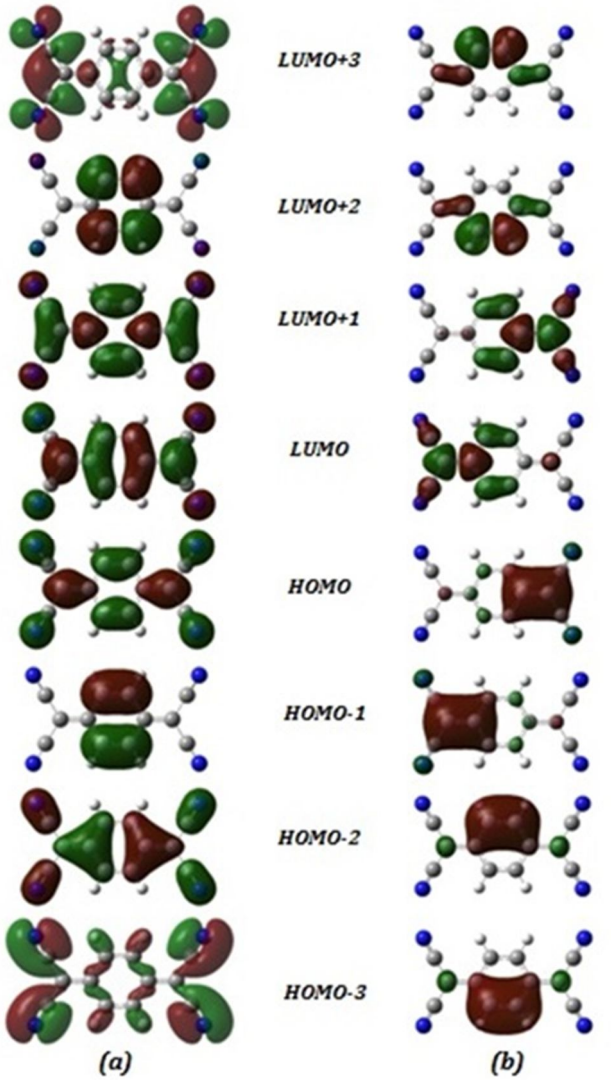

Figure 5 The frontier molecular orbitals (HOMOs and LUMOs); (a) ground state and (b) excited state of TCNQ molecule. The green and red colors represent the hole and electron, respectively.

3.8. UV-Visible analysis

The low-lying single excited states of the TCNQ molecule have been identified using ab initio CIS/6-31G(d) based on the completely optimized ground-state structure. Table 8 reports the results of the calculations for the the vertical excitation energies (eV), absorption maxima (λ_{max}) (nm) and oscillator strength (f). The Frank-Condon principle typically states that the greatest absorption peak- which are a function of the electron availability (λ_{max}) - in a UV-VIS spectrum corresponds to vertical excitation.

The apparent absorption maxima of this molecule correlate to the electronic transition between frontier orbitals, such as translation from HOMO to LUMO, according to calculations of the molecular orbital geometry. As can be seen from Table 8, the calculation predicts three electronic transitions. For the gas phase, the computed absorption maximum values are 345.73, 277.65 and 215.16 nm. One electronic excitation from the highest occupied molecular orbital to the lowest unoccupied molecular orbital primarily describes these electronic absorptions, which correspond to the transition from the ground to the first excited state. Table 8 also shows the oscillator strength and excitation energies. Figure 6 shows the UV-Vis spectrum of TCNQ molecule.

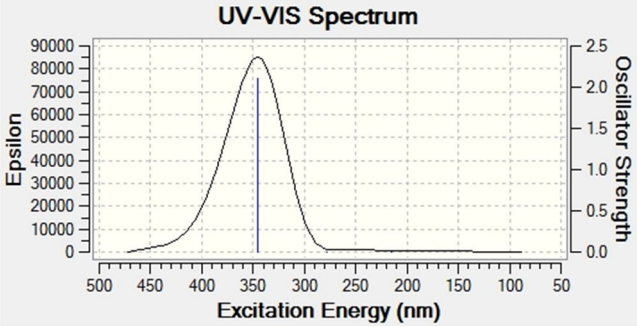

Figure 6 The calculated UV-Vis spectrum of TCNQ molecule by CIS/6-31G(d) method.

The bands at positions 215.16 and 277.65 nm, which have the shorter wavelength and higher energies, can be attributed to to the $\pi \rightarrow \pi^*$ intermolecular transition since the TCNQ molecule possesses $n \rightarrow \pi^*$ and $\pi \rightarrow \pi^*$ intermolecular transitatins (within TCNQ molecule), meanwhile the other bands located at and 345.73 nm, which has the higher wavelengths and lower energy, can be assigned to $n \rightarrow \pi^*$ the intramolecular transitions from the nitrogen atoms to the LUMO of the C=C (ring) π-bonds.

Table 8 The UV–Vis excitation energy (ΔE)and oscillator strength (f) for TCNQ molecule calculated by ab initio CIS/6-31G(d).

States	λ_{max} (nm)	Excitation energy (eV)	F
S1	345.73	3.5862	2.1036
S2	277.65	4.4655	0.0000
S3	215.16	5.7623	0.0000

4. Conclusion

In the current work , for the ground and excited states, respectively, the optimal molecular structures, vibrational frequencies and matching vibrational assignments, , ^{1}H, ^{13}C and ^{15}N NMR, natural atomic charge, thermodynamic parameters, NBO, frontier molecular orbitals and UV-Visible analysis of the TCNQ molecule have been computed using DFT/B3LYP/6-31G(d) and CIS/6-31G(d) methods for the ground and excited states, respectively. The ring geometry of the planar TCNQ molecule in S_1 is somewhat deformed from that of a perfect hexagon due to the excitation, according to the bond distance study for the title molecule. The NMR analysis shows that, The N atom's higher electronegativity feature causes it to polarize the electron distribution in its bond with the neighboring carbon atom, which lowers the electron density at the bridge of this named molecule. The DFT/B3LYP/6-31G(d) method is a good one for computations, as evidenced by a comparison of the title molecule's estimated vibrational frequencies with those found in the literature. The natural atomic charge study shows that, the TCNQ molecule become more acidic when it is in its ground state because the H9, H7, H10, H8, C3 and C6 atoms can accommodate higher positive charge. While, the excited state of TCNQ molecule causes the positive charge of C3 and C6 becomes less positive (+0.128e) charge. As a consequence of excitation, the TCNQ molecule becomes less acidic. The electron affinity of TCNQ molecule in the ground state is 4.84339 (eV) is high because TCNQ is a conjugated π –system that is flat, highly symmetrical, and contains four electron-withdrawing groups at different ends of the molecule. Because of the excitation effect, the NBO analysis reveals that the donor bonds' stabilization energy of the donor bonds (C1-C2) and (C4-C5) increased from 18.73 to become 29.83 kJ/mol. The fact that both the HOMOs and the LUMOs are primarily found on the rings suggests that the HOMO–LUMO orbitals are primarily of the the π-anti bonding kind. The electronic absorption correlates with the transition from the ground state to the first excited state, according to the UV-VIS study. Furthermore, a single electron excitation from the highest occupied molecular orbital to the lowest unoccupied molecular orbital mostly describes this absorption.

Data Availability

No data were used to support this study.

Conflicts of Interest

The authors declare that they have no conficts of interest.

How to Cite : Sabah Yahya Huthaily (2023). FT-IR, NMR spectral analysis and theoretical NBO, FMOs, UV-Vis analysis of 7,7',8,8'-tetracyanoquinodimethane (TCNQ) in its ground and excited states by DFT and CIS methods Certain results for the three- variable Srivastava polynomials with two parameters, *Abhath Journal of Basic and Applied Sciences*, 2(2), 1-14.

References

[1] **J. Fraxedas (2006)** Molecular Organic Materials From Molecules to Crystalline Solids, Cambridge University Press.

[2] **G. Horowitz (1998)** Adv. Mater., 10: 365-377.

[3] **H.E.A. Huitema; G.H. Gelinck; J.B.P.H. van der Putten; K.E. Kuijk; K.M. Hart; E. Cantatore; D.M. de Leeuw (2002)** Adv. Mater., 14: 1201-1204.

[4] **J.J.M. Halls; C.A. Walsh; N.C. Greenham; E.A. Marseglia; R.H. Friend; S.C. Moratti; A.B. Holmes (1995)** Nature, 376: 498-500.

[5] **C.J. Brabec; N.S. Sariciftci; J.C. Hummelen (2001)** Adv. Funct. Mater., 11: 15-26.

[6] **J.H. Schön; A. Dodabalapur; C. Kloc; B. Batlogg (2000)** Science, 290: 963-965.

[7] **J.H. Schön; H. Meng; Z. Bao (2001)** Nature, 413: 713-716.

[8] **X.D. Cui; A. Primak; X. Zarate; J. Tomfohr; O.F. Sankey; A.L. Moore; T.A. Moore; D. Gust; G. Harris; S.M. Lindsay (2001)** Science, 204: 571-574.

[9] **R.M. Metzger (1999)** Acc. Chem. Res., 32: 950-957.

[10] **M. Goes; J.W. Verhoeven; H. Hofstraat; K. Brunner (2003)** Chem. Phys. Chem., 4: 349–358.

[11] **T.T. Wooster; M. Watanabe; R.W. Murray (1992)** J. Phys. Chem., 96: 5886-5893.

[12] **K. Okamoto; M. Ozeki; A. Itaya; S. Kusabayashi; H. Mikawa (1975)** Bull. Chem. Soc. Jpn., 48: 1362-1367.

[13] **J.M. Pearson (1977)** Pure Appl. Chem., 49: 463–477.

[14] **J. Guillet (1985)** In Polymer Photophysics and Photochemistry: An Introduction to the Study of Photoprocesses in Macromolecules; Cambridge University Press: Cambridge, U.K.

[15] **S. Sugunan; C.G. Ramankutty (1995)** J. Chemical and Engineering Data, 40(2): 417–418.

[16] **A.D. Becke (1993)** J. Chem. Phys., 98: 5648–5652.

[17] **C. Lee; W. Yang; R.G. Parr** (1988) Phys. Rev., B37: 785–789.

[18] **J.P. Perdew; Y. Wang; (1986)** Phys. Rev., B33: 8800–8802.

[19] **A. Frisch; A.B. Nielsen; A.J. Holder (2000)** Gaussview Users Manual, Gaussian Inc., Pittsburg, PA, 2000.

[20] **J.B. Foresman; M. Head-Gordon; J.A. Pople; M.J. Frisch (1992)** J. Phys. Chem., 96: 135-149.

[21] **G. Orlandi; P. Palmieri; R. Tarroni; F. Zerbetto; M.Z. Zgierski (1994)** J. Chem. Phys., 100: 2458-2464.

[22] **M.J. Frisch; G.W. Trucks; H.B. Schlegel; G.E. Scuseria; M.A. Robb; J.R. Cheeseman; J.A. Montgomery; Jr. T.**

Vreven; K.N. Kudin; J.C. Burant; J.M. Millam; S.S. Iyengar; J. Tomasi; V. Barone; B. Mennucci; M. Cossi; G. Scalmani; N. Rega; G.A. Petersson; H. Nakatsuji; M. Hada; M. Ehara; K. Toyota; R. Fukuda; J. Hasegawa; M. Ishida; T. Nakajima; Y. Honda; O. Kitao; H. Nakai; M. Klene; X. Li; J.E. Knox; H.P. Hratchian; J.B. Cross; C. Adamo; J. Jaramillo; R. Gomperts; R.E. Stratmann; O. Yazyev; A.J. Austin; R. Cammi; C. Pomelli; J.W. Ochterski; P.Y. Ayala; K. Morokuma; G.A. Voth; P. Salvador; J.J. Dannenberg; V.G. Zakrzewski; S. Dapprich; A.D. Daniels; M.C. Strain; O. Farkas; D.K. Malick; A.D. Rabuck; K. Raghavachari; J.B. Foresman; J.V. Ortiz; Q. Cui; A.G. Baboul; S. Clifford; J. Cioslowski; B.B. Stefanov; G. Liu; A. Liashenko; P. Piskorz; I. Komaromi; R.L. Martin; D.J. Fox; T. Keith; M.A. Al-Laham; C.Y. Peng; A. Nanayakkara; M. Challacombe; P.M. W. Gill; B. Johnson; W. Chen; M.W. Wong; C. Gonzalez; J.A. Pople; Gaussian 03, Revision E.01 (2004), Inc., Wallingford, CT.

[23] **E.D. Glendening; A.E. Reed; J.E. Carpenter; F. Weinhold ,NBO Version 3.1 TCI (1998),** University of Wisconsin, Madison.

[24] **R. E. Long; R. A. Sparks; K. N. Trueblood (1965)** Acta Cryst., 18: 932-939.

[25] **D.V. Ziolkovskiy; A.V. Kravchenko; V.A. Starodub; O.N. Kazheva; A.V. Khotkevich (2005)** Func. Mate., 12(3): 577-582.

[26] **M.M. El-Nahass; M.A. Kamel; A.F. El-deeb; A.A. Atta; S.Y. Huthaily (2011)** Spectrochimica Acta A, 79: 443–450.

[27] **S. Ayyappan; N. Sundaraganesan; V. Aroulmoji; E. Murano; S. Sebastian (2010)** Spectrochim. Acta A, 77: 264–275.

[28] **K. Wolinski; J.F. Hinton; P. Pulay (1990)** J. Am. Chem. Soc., 112: 8251–8260.

[29] **R. Ditchfield (1972)** Molecular Orbital Theory of Magnetic Shielding and Magnetic Susceptibility, 56: 5688-5691.

[30] **N. Subramanian; N. Sundaraganesan; J. Jayabharathi (2010)** Spectrochim. Acta A, 76: 259–269.

[31] **N. Sundaraganesana; E. Kavithaa, S. Sebastiana; J.P. Cornardb; M. Martel (2009)** Spectrochim. Acta Part A, 74: 788–797.

[32] **G. Varsanyi (1974)** Assignments of Vibrational Spectra of Seven Hundred Benzene Derivatives, Wiley, New York.

[33] **G. Varsanyi; S. Szoke (1969)** Vibrational Spectra of Benzene Derivatives, Academic Press, New York.

[34] **J.B. Lambert; H.F. Shurvell; L. Verbit; R.G. Cooks, G.H. Stout (1976)** Organic Structural Analysis, Macmillan Publ. Co. Inc., New York.

[35] **N. Sundaraganesan; S. Kalaichelvan; C. Meganathan; B.D. Jashua (2008)** Spectrochim. Acta A, 71: 898–906.

[36] **M. Silverstein; G.C. Basseler; C. Morill (1981)** Spectrometric Identification of Organic Compounds, Wiley, New York.

[37] **N. M. Aghatabay; M. Tulu; M. Somer; D. Haciu; A. Yilmaz (2008)** Struct. Chem., 19: 21–32.

[38] **L.J. Bellamy (1959)** The Infrared Spectra of Complex Molecules, John Wiley, New York.

[39] **N. Sundaraganesana; C. Meganathana; B. Dominic Joshuaa; P. Mani; A. Jayaprakash (2008)** Spectrochim. Acta A, 71: 1134–1139.

[40] **N.P.G. Roeges (1994)** A Guide to the Complete Interpretation of Infrared Spectra of Organic Structures, Wiley, New York.

[41] **J.R. Durig; J.F. Sullivan; G.M. Attia (1986)** Spectrochim. Acta, 42 (2): 75-88.

[42] **J.R. Durig; G.A. Guirgis; K.A. Krutules; h. phan, H.D. Stidham (1994)** J. Raman Spectrosc., 25: 221-232.

[43] **L.X. Hong; Z.X. Zhou (2010)** J. Mol. Struct. (THEOCHEM), 957: 15–20.

[44] **N.S. Allen (2010)** Photochemistry and Photophysics of Polymer Materials, Wiley, New York.

[45] **M.A. Palafox (2000)** Int. J. Quantum Chem., 77: 661-684.

[46] **J. M. Seminario (2007)** Molecular and Nano Electronics:Analysis, Design and Simulation, Elsevier, UK.

[47] **R. Kanakaraju; P. Kolandaivel (2003)** J. Mol. Struct. (THEOCHEM), 623: 39–49.

[48] **C. Clean (2002)** Synthesis of Heterocyclic Analogues of Benzo-TCNQ, Ph. D. Thesis.

[49] **M. Szafran; A. Komasa; E.B. Adamska (2007)** J. Mol. Struct. (THEOCHEM), 827: 101-107.

[50] **S. Sebastian; N. Sundaragnesan (2010)** Spectrochim. Acta A, 75: 941-952.

[51] **I. Fleming** (1976) Frontier Orbitals and Organic Chemical Reactions, John Wiley and Sons, New York.

[52] **K. Fukui (1975)** Theory of Orientation and Stereoselection, Springer-Verlag, Berlin.

[53] **N. Özdemir; M. Dinçer; İ. Koca; O. Büyükgüngör (2009)** J. Mol. Model., 15: 1193–1201.

Appendix

Table 3 Theoretical assignments of the vibrational modes of TCNQ Ground state.

Vibrational mode	Wavenumber (cm^{-1})	Red. Mass	Frc constant	IR intensity	Temperature (K)	Species	Vibration assignment
ν_1	47.00695	8.7673	0.0124	9.1989	70.3900	A''	Lattice vibration (butterfly)
ν_2	48.17711	13.5354	0.0201	0.0000	72.1400	A''	γ(t) NCCCN
ν_3	82.13168	12.4207	0.0535	5.1213	122.9900	A'	Lattice vibration (butterfly)
ν_4	111.6536	4.1275	0.0328	0.0000	167.2000	A''	Lattice vibration (butterfly)
ν_5	114.4504	13.8742	0.1160	0.0000	171.3900	A'	β(s) NCCCN
ν_6	131.5546	10.6482	0.1176	0.0000	197.0000	A'	Lattice vibration (butterfly)
ν_7	135.4657	12.4595	0.1459	8.4554	202.8600	A'	β(s) NCCCN
ν_8	143.3070	8.8341	0.1158	0.0003	214.6000	A''	Lattice vibration (butterfly)
ν_9	210.8120	9.4800	0.2689	11.9595	315.6900	A''	Lattice vibration (butterfly)
ν_{10}	279.2787	9.9544	0.4955	0.0018	418.2100	A'	Lattice vibration (butterfly)
ν_{11}	294.7709	6.9214	0.3838	0.0004	441.4100	A''	Lattice vibration (butterfly)
ν_{12}	325.3899	12.1335	0.8199	0.0000	487.2600	A'	Lattice vibration (butterfly)
ν_{13}	365.7454	6.5162	0.5563	0.0000	547.7000	A'	Lattice vibration (butterfly)
ν_{14}	385.0637	4.9125	0.4649	0.0000	576.6200	A''	γ(ω) CCC
ν_{15}	421.7900	10.8404	1.2309	0.0062	631.6200	A''	γ(t) CCC
ν_{16}	452.7954	4.9451	0.6471	0.0000	678.0500	A''	γ(t) CCC
ν_{17}	465.9297	3.0167	0.4180	16.7951	697.7200	A''	γ(ω) CCC
ν_{18}	501.2849	11.1844	1.7324	0.0103	737.4300	A'	β(ρ) CCC
ν_{19}	516.4906	7.0441	1.1993	0.0001	773.4300	A'	Lattice vibration (butterfly)
ν_{20}	542.1192	7.7879	1.4608	3.9527	811.8100	A'	Lattice vibration (butterfly)
ν_{21}	594.9410	12.3462	2.7891	0.0000	890.9100	A'	β(s) CCC
ν_{22}	595.9928	12.4318	2.8184	0.1900	892.4900	A'	β(s) CCC
ν_{23}	618.7186	7.2090	1.7641	0.0000	926.5200	A'	β(ρ) CCC
ν_{24}	630.3350	7.6447	1.9386	0.0004	943.9100	A''	γ(ω) CCC
ν_{25}	681.6670	4.4037	1.3060	6.5968	1020.7800	A''	γ(ω) CH
ν_{26}	706.1195	7.6597	2.4375	0.0000	1057.4000	A'	β(s) CCC
ν_{27}	780.8865	5.6563	2.2014	0.0000	1169.3600	A''	γ(ω) CCC
ν_{28}	805.2704	1.2816	0.5304	0.0001	1205.8700	A''	γ(ω) CH
ν_{29}	869.2360	1.9199	0.9259	64.6637	1301.6600	A''	γ(ω) CH
ν_{30}	943.2986	8.8135	5.0053	0.0000	1412.5700	A'	Ring breathing
ν_{31}	962.6444	2.7519	1.6276	0.8251	1441.5400	A'	β(s) CCC
ν_{32}	986.6320	8.5888	5.3362	0.0298	1477.4600	A'	β(s) CCC
ν_{33}	999.7697	1.3322	0.8499	0.0000	1497.1300	A''	γ(t) CH
ν_{34}	1008.784	1.3303	0.8640	0.0000	1510.6300	A''	γ(t) CH
ν_{35}	1100.543	2.9344	2.2684	13.9858	1648.0400	A'	υ_{as} CC+ β(s) CH
ν_{36}	1168.031	7.6814	6.6886	0.0000	1749.1000	A'	υ_{as} CC
ν_{37}	1199.689	2.2132	2.0330	3.9783	1796.5100	A'	υ_{as} CC
ν_{38}	1215.309	1.1425	1.0770	0.0000	1819.9000	A'	β(s) CH
ν_{39}	1320.507	1.8881	2.1013	0.0000	1977.4300	A'	υ_{as} CC+ β(s) CH
ν_{40}	1346.967	3.1724	3.6736	8.3965	2017.0500	A'	υ_{as} CC
ν_{41}	1397.149	1.8223	2.2828	1.4634	2092.2000	A'	υ_{as} CC+ β(s) CH
ν_{42}	1435.868	2.8267	3.7196	0.0000	2150.1800	A'	υ_{as} CC
ν_{43}	1442.501	9.5546	12.6890	0.0000	2160.1100	A'	υ CC
ν_{44}	1535.313	4.6073	6.9315	58.9131	2299.1000	A'	υ_{as} CC
ν_{45}	1544.066	6.2526	9.5142	14.0751	2312.2000	A'	υ_{as} CC
ν_{46}	1617.204	5.6040	9.3543	0.0000	2421.7200	A'	υ CC
ν_{47}	2186.093	12.6529	38.5934	1.3946	3273.6200	A'	υ_{as} C≡N
ν_{48}	2186.147	12.6531	38.5959	0.0003	3273.7000	A'	υ_{as} C≡N
ν_{49}	2199.337	12.6587	39.0803	0.0000	3293.4600	A'	υ C≡N
ν_{50}	2201.317	12.6593	39.1524	83.4023	3296.4200	A'	υ C≡N
ν_{51}	3096.827	1.0871	6.6543	0.0234	4637.4300	A'	υ_{as} CH
ν_{52}	3096.883	1.0886	6.6637	1.6554	4637.5100	A'	υ_{as} CH
ν_{53}	3111.691	1.0964	6.7754	0.8167	4659.6800	A'	υ CH
ν_{54}	3113.828	1.0984	6.7974	0.0000	4662.8800	A'	υ CH

υ: symmetric stretching; υ_{as}: asymmetric stretching; β: in-plane-bending; γ: out-of-plane bending; s: scissoring; ω: wagging; ρ: rocking; t: twisting.

Table 6 a Second order perturbation theory analysis of Fock matrix in NBO basis for TCNQ in its ground state.

Donor (i)	Type	ED/e	Acceptor(j)	Type	ED/e	$E^{(2)}$ (kJmol−1)	E(j)−E(i) (a.u.)	F (i, j) (a.u.)
C1-C2	σ	1.98093	C1-C6	σ^*	0.02412	2.73	1.22	0.052
			C1-H7		0.01291	1.87	1.21	0.043
			C2-C3		0.02412	2.73	1.22	0.052
			C2-H8		0.01291	1.87	1.21	0.043
			C3-C12		0.03040	2.46	1.30	0.051
			C6-C11		0.03040	2.46	1.30	0.051
C1-C2	π	1.79211	C3-C12	π^*	0.31639	18.73	0.28	0.067
			C6-C11		0.31639	18.73	0.28	0.067
C1-C6	σ	1.97267	C1 - C2	σ^*	0.01218	2.65	1.31	0.053
			C1 - H7		0.01291	0.90	1.16	0.029
			C2 - H8		0.01291	2.41	1.16	0.047
			C5 - C6		0.02412	2.18	1.17	0.045
			C5 -H10		0.01291	1.74	1.16	0.040
			C6 -C11		0.03040	3.60	1.25	0.060
			C11 -C14		0.03449	3.19	1.20	0.055
C1-H7	σ	1.97846	C1-C2	σ^*	0.01218	1.88	1.15	0.042
			C1-C6		0.02412	0.61	1.01	0.022
			C2-C3		0.02412	4.77	1.01	0.062
			C5-C6		0.02412	3.61	1.01	0.054
C2-C3	σ	1.97267	C1-C2	σ^*	0.01218	2.65	1.31	0.053
			C1-H7		0.01291	2.41	1.16	0.047
			C2-H8		0.01291	0.90	1.16	0.029
			C3-C4		0.02412	2.18	1.17	0.045
			C3-C12		0.03040	3.60	1.25	0.060
			C4-H9		0.01291	1.74	1.16	0.040
			C12-C15		0.03448	3.19	1.20	0.055
C2 - H8	σ	1.97846	C1-C2	σ^*	0.01218	1.88	1.15	0.042
			C1-C6		0.02412	4.77	1.01	0.062
			C2-C3		0.02412	0.61	1.01	0.022
			C3-C4		0.02412	3.61	1.01	0.054
C3-C4	σ	1.97267	C2-C3	σ^*	0.02412	2.18	1.17	0.045
			C2-H8		0.01291	1.74	1.16	0.040
			C3-C12		0.03040	3.60	1.25	0.060
			C4-C5		0.01218	2.65	1.31	0.053
			C4-H9		0.01291	0.90	1.16	0.029
			C5-H10		0.01291	2.41	1.16	0.047
			C12-C16		0.03449	3.19	1.20	0.055
C3-C12	σ	1.96536	C1-C2	σ^*	0.01218	1.16	1.36	0.036
			C2-C3		0.02412	2.98	1.22	0.054
			C3-C4		0.02412	2.98	1.22	0.054
			C4-C5		0.01218	1.16	1.36	0.036
			C12-C15		0.03448	4.02	1.26	0.064
			C12-C16		0.03449	4.02	1.26	0.064
			C15-N19		0.00964	4.37	1.58	0.075
			C15-N19	π^*	0.01628	0.98	0.83	0.026
			C16-N20	σ^*	0.00964	4.37	1.58	0.075
			C16-N20	π^*	0.01628	0.98	0.83	0.026
C3-C12	π	1.70619	C1-C2	π^*	0.13238	12.84	0.31	0.059
			C4-C5		0.13238	12.84	0.31	0.059
			C15-N19		0.08576	18.61	0.37	0.078
			C16-N20		0.08575	18.61	0.37	0.078
C4-C5	σ	1.98093	C3-C4	σ^*	0.02412	2.73	1.22	0.052
			C3-C12		0.03040	2.46	1.30	0.051
			C4-H9		0.01291	1.87	1.21	0.043
			C5-C6		0.02412	2.73	1.22	0.052
			C5-H10		0.01291	1.87	1.21	0.043
			C6-C11		0.03040	2.46	1.30	0.051

Donor (i)	Type	ED/e	Acceptor(j)	Type	ED/e	$E^{(2)}$ (kJmol−1)	E(j)−E(i) (a.u.)	F (i, j) (a.u.)
C4-C5	π	1.79210	C3-C12	π^*	0.31639	18.73	0.28	0.067
			C6-C11		0.31639	18.73	0.28	0.067
C4-H9	σ	1.97846	C2-C3	σ^*	0.02412	3.61	1.01	0.054
			C3-C4		0.02412	0.61	1.01	0.022
			C4-C5		0.01218	1.88	1.15	0.042
			C5-C6		0.02412	4.77	1.01	0.062
C5-C6	σ	1.97267	C1-C6	σ^*	0.02412	2.18	1.17	0.045
			C1-H7		0.01291	1.74	1.16	0.040
			C4-C5		0.01218	2.65	1.31	0.053
			C4-H9		0.01291	2.41	1.16	0.047
			C5-H10		0.01291	0.90	1.16	0.029
			C6-C11		0.03040	3.60	1.25	0.060
			C11-C13		0.03449	3.19	1.20	0.055
C5-H10	σ	1.97846	C1-C6	σ^*	0.02412	3.61	1.01	0.054
			C3-C4		0.02412	4.77	1.01	0.062
			C4-C5		0.01218	1.88	1.15	0.042
			C5-C6		0.02412	0.61	1.01	0.022
C6-C11	σ	1.96536	C1-C2	σ^*	0.01218	1.16	1.36	0.036
			C1-C6		0.02412	2.98	1.22	0.054
			C4-C5		0.01218	1.16	1.36	0.036
			C5-C6		0.02412	2.98	1.22	0.054
			C11-C13		0.03449	4.02	1.26	0.064
			C11-C14		0.03449	4.02	1.26	0.064
			C13-N17		0.00964	4.37	1.58	0.075
			C13-N17		0.01628	0.98	0.83	0.026
			C14-N18		0.00964	4.37	1.58	0.075
			C14-N18	π^*	0.01628	0.98	0.83	0.026
C6-C11	π	1.70619	C1-C2	π^*	0.13238	12.84	0.31	0.059
			C4-C5		0.13238	12.84	0.31	0.059
			C13-N17		0.08576	18.61	0.37	0.078
			C14-N18		0.08575	18.60	0.37	0.078
C11-C13	σ	1.97329	C5-C6	σ^*	0.02412	3.17	1.22	0.056
			C6-C11		0.03040	3.87	1.30	0.063
			C11-C14		0.03449	2.19	1.26	0.047
			C13-N17		0.00964	6.08	1.58	0.088
			C14-N18		0.00964	3.53	1.58	0.067
			C14-N18	π^*	0.01628	2.47	0.83	0.040
C11-C14	σ	1.97329	C1-C6	σ^*	0.02412	3.17	1.22	0.056
			C6-C11		0.03040	3.87	1.30	0.063
			C11-C13		0.03449	2.19	1.26	0.047
			C13-N17		0.00964	3.53	1.58	0.067
			C13-N17	π^*	0.01628	2.47	0.83	0.041
			C14-N18	σ^*	0.00964	6.08	1.58	0.088
C12-C15	σ	1.97329	C2-C3	σ^*	0.02412	3.17	1.22	0.056
			C3-C12		0.03040	3.87	1.30	0.063
			C12-C16		0.03449	2.19	1.26	0.047
			C15-N19		0.00964	6.08	1.58	0.088
			C16-N20		0.00964	3.53	1.58	0.067
			C16-N20	π^*	0.01628	2.47	0.83	0.041
C12-C16	σ	1.97329	C3-C4	σ^*	0.02412	3.17	1.22	0.056
			C3-C12		0.03040	3.87	1.30	0.063
			C12-C15		0.03448	2.19	1.26	0.047
			C15-N19		0.00964	3.53	1.58	0.067
			C15-N19	π^*	0.01628	2.47	0.83	0.040
			C16-N20	σ^*	0.00964	6.08	1.58	0.088
C13-N17	σ	1.99527	C11-C13	σ^*	0.03449	6.81	1.56	0.093
	π	1.98166	C6-C11		0.03040	3.08	0.90	0.047
			C11-C14		0.03449	3.74	0.85	0.051
		1.93816	C6-C11	σ^*	0.31639	9.65	0.34	0.055
C14-N18	σ	1.99527	C11-C14	σ^*	0.03449	6.81	1.56	0.093

Donor (i)	Type	ED/e	Acceptor(j)	Type	ED/e	$E^{(2)}$ (kJmol−1)	E(j)−E(i) (a.u.)	F (i, j) (a.u.)
	π	1.98166	C6-C11		0.03040	3.08	0.90	0.047
			C11-C13		0.03449	3.74	0.85	0.051
		1.93815	C6-C11	π^*	0.31639	9.65	0.34	0.055
C15-N19	σ	1.99527	C12-C15	σ^*	0.03448	6.81	1.56	0.093
	π	1.98166	C3-C12		0.03040	3.08	0.90	0.047
			C12-C16		0.03449	3.74	0.85	0.051
		1.93816	C3-C12	π^*	0.31639	9.65	0.34	0.055
C16-N20	σ	1.99527	C12-C16	σ^*	0.03449	6.81	1.56	0.093
	π	1.98166	C3-C12		0.03040	3.08	0.90	0.047
			C12-C15		0.03448	3.74	0.85	0.051
		1.93815	C3-C12	π^*	0.31639	9.65	0.34	0.055
N17 (LP)	n	1.96901	C11-C13	σ^*	0.03449	12.68	1.01	0.101
N18 (LP)	n	1.96901	C11-C14	σ^*	0.03449	12.68	1.01	0.101
N19 (LP)	n	1.96901	C12-C15	σ^*	0.03448	12.68	1.01	0.101
N20 (LP)	n	1.96901	C12-C16	σ^*	0.03449	12.68	1.01	0.101

Table 6b Second order perturbation theory analysis of Fock matrix in NBO basis for TCNQ in its excited state

Donor (i)	Type	ED/e	Acceptor(j)	Type	ED/e	$E^{(2)}$ (kJmol^{-1})	E(j)−E(i) (a.u.)	F (i, j) (a.u.)
C1-C2	σ	1.98002	C1-C6	σ^*	0.02183	4.03	1.74	0.075
			C1-H7		0.01096	2.75	1.74	0.062
			C2-C3		0.02183	4.03	1.74	0.075
			C2-H8		0.01096	2.75	1.74	0.062
			C3-C12		0.02884	3.32	1.78	0.069
			C6-C11		0.02884	3.32	1.78	0.069
C1-C2	π	1.82859	C3-C12	π^*	0.24072	29.83	0.52	0.113
			C6-C11		0.24072	29.83	0.52	0.113
C1-C6	σ	1.97401	C1 - C2	σ^*	0.01294	3.70	1.81	0.073
			C1 - H7		0.01096	1.59	1.69	0.046
			C2 - H8		0.01096	2.65	1.69	0.060
			C5 - C6		0.02183	3.63	1.69	0.070
			C5 -H10		0.01096	2.36	1.69	0.057
			C6 -C11		0.02884	4.75	1.72	0.081
			C11 -C14		0.02841	3.43	1.74	0.069
C1-H7	σ	1.97980	C1-C2	σ^*	0.01294	3.05	1.61	0.063
			C1-C6		0.02183	1.42	1.49	0.041
			C2-C3		0.02183	5.93	1.49	0.084
			C5-C6		0.02183	4.80	1.49	0.076
C2-C3	σ	1.97401	C1-C2	σ^*	0.01294	3.70	1.81	0.073
			C1-H7		0.01096	2.65	1.69	0.060
			C2-H8		0.01096	1.59	1.69	0.046
			C3-C4		0.02183	3.63	1.69	0.070
			C3-C12		0.02884	4.75	1.72	0.081
			C4-H9		0.01096	2.36	1.69	0.057
			C12-C15		0.02841	3.43	1.74	0.069
C2 - H8	σ	1.97980	C1-C2	σ^*	0.01294	3.05	1.61	0.063
			C1-C6		0.02183	5.93	1.49	0.084
			C2-C3		0.02183	1.42	1.49	0.041
			C3-C4		0.02183	4.80	1.49	0.076
C3-C4	σ	1.97401	C2-C3	σ^*	0.02183	3.63	1.69	0.070
			C2-H8		0.01096	2.36	1.69	0.057
			C3-C12		0.02884	4.75	1.72	0.081
			C4-C5		0.01294	3.70	1.81	0.073
			C4-H9		0.01096	1.59	1.69	0.046
			C5-H10		0.01096	2.65	1.69	0.060
			C12-C16		0.02841	3.43	1.74	0.069
C3-C12	σ	1.96684	C1-C2	σ^*	0.01294	1.64	1.85	0.049

Donor (i)	Type	ED/e	Acceptor(j)	Type	ED/e	$E^{(2)}$ ($kJmol^{-1}$)	E(j)−E(i) (a.u.)	F (i, j) (a.u.)
			C2-C3		0.02183	4.13	1.72	0.076
			C3-C4		0.02183	4.13	1.72	0.076
			C4-C5		0.01294	1.64	1.85	0.049
			C12-C15		0.02841	5.28	1.77	0.086
			C12-C16		0.02841	5.28	1.77	0.086
			C15-N19		0.01138	5.40	2.17	0.097
			C15-N19	π^*	0.01030	1.60	1.27	0.040
			C16-N20	σ^*	0.01138	5.40	2.17	0.097
			C16-N20	π^*	0.01030	1.60	1.27	0.040
C3-C12	π		C1-C2	π^*	0.09899	18.26	0.56	0.093
			C4-C5		0.09899	18.26	0.56	0.093
			C15-N19		0.06966	28.59	0.66	0.128
			C16-N20		0.06966	28.59	0.66	0.128
C4-C5	σ	1.98002	C3-C4	σ^*	0.02183	4.03	1.74	0.075
			C3-C12		0.02884	3.32	1.78	0.069
			C4-H9		0.01096	2.75	1.74	0.062
			C5-C6		0.02183	4.03	1.74	0.075
			C5-H10		0.01096	2.75	1.74	0.062
			C6-C11		0.02884	3.32	1.78	0.069
C4-C5	π	1.82859	C3-C12	π^*	0.24072	29.83	0.52	0.113
			C6-C11		0.24072	29.83	0.52	0.113
C4-H9	σ	1.97980	C2-C3	σ^*	0.02183	4.80	1.49	0.076
			C3-C4		0.02183	1.42	1.49	0.041
			C4-C5		0.01294	3.05	1.61	0.063
			C5-C6		0.02183	5.93	1.49	0.084
C5-C6	σ	1.97401	C1-C6	σ^*	0.02183	3.63	1.69	0.070
			C1-H7		0.01096	2.36	1.69	0.057
			C4-C5		0.01294	3.70	1.81	0.073
			C4-H9		0.01096	2.65	1.69	0.060
			C5-H10		0.01096	1.59	1.69	0.046
			C6-C11		0.02884	4.75	1.72	0.081
			C11-C13		0.02841	3.43	1.74	0.069
C5-H10	σ	1.97980	C1-C6	σ^*	0.02183	4.80	1.49	0.076
			C3-C4		0.02183	5.93	1.49	0.084
			C4-C5		0.01294	3.05	1.61	0.063
			C5-C6		0.02183	1.42	1.49	0.041
C6-C11	σ	1.96684	C1-C2	σ^*	0.01294	1.64	1.85	0.049
			C1-C6		0.02183	4.13	1.72	0.076
			C4-C5		0.01294	1.64	1.85	0.049
			C5-C6		0.02183	4.13	1.72	0.076
			C11-C13		0.02841	5.28	1.77	0.086
			C11-C14		0.02841	5.28	1.77	0.086
			C13-N17		0.01138	5.40	2.17	0.097
			C13-N17	π^*	0.01030	1.60	1.27	0.040
			C14-N18	σ^*	0.01138	5.40	2.17	0.097
			C14-N18	π^*	0.01030	1.60	1.27	0.040
C6-C11	π	1.76269	C1-C2	π^*	0.09899	18.26	0.56	0.093
			C4-C5		0.09899	18.26	0.56	0.093
			C13-N17		0.06966	28.59	0.66	0.128
			C14-N18		0.06966	28.59	0.66	0.128
C11-C13	σ	1.97284	C5-C6	σ^*	0.02183	3.48	1.74	0.070
			C6-C11		0.02884	4.97	1.77	0.084
			C11-C14		0.02841	3.42	1.79	0.070
			C13-N17		0.01138	11.31	2.18	0.141
			C14-N18		0.01138	4.73	2.18	0.091
			C14-N18		0.01030	2.58	1.28	0.052
C11-C14	σ	1.97284	C1-C6	σ^*	0.02183	3.48	1.74	0.070
			C6-C11		0.02884	4.97	1.77	0.084
			C11-C13		0.02841	3.42	1.79	0.070
			C13-N17		0.01138	4.73	2.18	0.091

Donor (i)	Type	ED/e	Acceptor(j)	Type	ED/e	$E^{(2)}$ ($kJmol^{-1}$)	E(j)−E(i) (a.u.)	F (i, j) (a.u.)
			C13-N17	π^*	0.01030	2.58	1.28	0.052
			C14-N18	σ^*	0.01138	11.31	2.18	0.141
C12-C15	σ	1.97284	C2-C3	σ^*	0.02183	3.48	1.74	0.070
			C3-C12		0.02884	4.97	1.77	0.084
			C12-C16		0.02841	3.42	1.79	0.070
			C15-N19		0.01138	11.31	2.18	0.141
			C16-N20	π^*	0.01138	4.73	2.18	0.091
			C16-N20	σ^*	0.01030	2.58	1.28	0.052
C12-C16	σ	1.97284	C3-C4	σ^*	0.02183	3.48	1.74	0.070
			C3-C12		0.02884	4.97	1.77	0.084
			C12-C15		0.02841	3.42	1.79	0.070
			C15-N19		0.01138	4.73	2.18	0.091
			C15-N19	π^*	0.01030	2.58	1.28	0.052
			C16-N20	σ^*	0.01138	11.31	2.18	0.141
C13-N17	σ	1.99346	C11-C13	σ^*	0.02841	10.93	2.20	0.139
C13-N17	π	1.98552	C6-C11		0.02884	4.13	1.27	0.065
			C11-C14		0.02841	4.84	1.28	0.071
			C14-N18	π^*	0.01030	0.52	0.78	0.018
C13-N17	σ	1.96074	C6-C11		0.24072	12.31	0.62	0.082
C14-N18	σ	1.99346	C11-C14	σ^*	0.02841	10.93	2.20	0.139
C14-N18	π	1.98552	C6-C11		0.02884	4.13	1.27	0.065
			C11-C13		0.02841	4.84	1.28	0.071
			C13-N17	π^*	0.01030	0.52	0.78	0.018
C14-N18	σ	1.96074	C6-C11		0.24072	12.31	0.62	0.082
C15-N19	σ	1.99346	C12-C15	σ^*	0.02841	10.93	2.20	0.139
C15-N19	π	1.98552	C3-C12		0.02884	4.13	1.27	0.065
			C12-C16		0.02841	4.84	1.28	0.071
			C16-N20	π^*	0.01030	0.52	0.78	0.018
C15-N19	σ	1.96074	C3-C12		0.24072	12.31	0.62	0.082
C16-N20	σ	1.99346	C12-C16	σ^*	0.02841	10.93	2.20	0.139
C16-N20	π	1.98552	C3-C12		0.02884	4.13	1.27	0.065
			C12-C15		0.02841	4.84	1.28	0.071
			C15-N19	π^*	0.01030	0.52	0.78	0.018
C16-N20	σ	1.96074	C3-C12		0.24072	12.31	0.62	0.082
N17 (*LP*)	n	1.97356	C11-C13	σ^*	0.02841	13.52	1.51	0.128
N18 (*LP*)	n	1.97356	C11-C14	σ^*	0.02841	13.52	1.51	0.128
N19 (*LP*)	n	1.97356	C12-C15	σ^*	0.02841	13.52	1.51	0.128
N20 (*LP*)	n	1.97356	C12-C16	σ^*	0.02841	13.52	1.51	0.128